Discovery of the Quiescent Body that Functions as a Biological Timer for Growth Resumption of Non-growing Bacterial Cells

Jiayu Yu[1†], Yang Liu[1†] & Zengyi Chang[1,2,*]

[1]The State Key Laboratory of Protein and Plant Gene Research, School of Life Sciences, Peking University, Beijing 100871, P.R. China
[2]Center for Protein Science, Peking University, Beijing 100871, P.R. China
[†]J.Y. and Y.L. contributed equally to this work
[*]Correspondence: changzy@pku.edu.cn (Z.C.)

Abstract

Bacterial cells in natural environment often exist in a non-growing state. They recover after a short or long lag time when encountering a growth-supportive condition. Such dormant bacteria are known for their high tolerance towards adverse conditions such as the presence of antibiotics and are thus viewed as a great challenge for the treatment of infectious diseases. Nevertheless, it remains poorly understood on how bacterial cells enter such an inert state and why a heterogeneous lag time is taken before they could recover. In this study, we accidentally discovered a subcellular structure that we term quiescent body, which is formed in the non-growing/non-dividing stationary-phase *E. coli* cells and selectively sequesters many proteins essential for cell growth, division and metabolism. This finding was made when we tried to trace the status of FtsZ, an essential protein for bacterial cytokinesis, via *in vivo* protein photo-crosslinking and live-cell fluorescence microscopic imaging. We further demonstrated the following. 1. Formation of quiescent bodies can be induced by indole and relies on the occurrence of cellular respiration. 2. When the non-growing cells are placed in fresh culture medium, the quiescent bodies will initiate their dissolution in cells that have started to re-grow, releasing the sequestered proteins for functional resumption, but remain unaltered in cells that have not yet started their re-growth. 3. Both the formation and dissolution of quiescent bodies occur in a highly heterogeneous manner among individual cells, and that the degree of their formation is highly correlated with the duration of the lag time taken for bacterial cells to recover. These findings strongly implicate that the quiescent bodies function as a biological timer for growth resumption of the non-growing cells. The maintenance of quiescent body possibly represents a distinguishing feature and is thus helpful for an unequivocal identification of such hitherto elusive dormant (persister) bacterial cells. Our findings shed light not only on how and why a lag time is taken, but also on inventing new ways to eradicate the multidrug-tolerant pathogens, for

example, by blocking the formation or promoting the dissolution of quiescent bodies in them.

Introduction

Bacterial cells in the natural environment are considered to mainly exist in a non-growing/non-dividing dormant state. One remarkable feature of such inert cells is their capacity to survive under adverse conditions, such as the high temperature (i.e., boiling) or the presence of any antibiotic[1–3]. Meanwhile, it has long been recognized that the non-growing/non-dividing bacterial cells commonly take a lag time, heterogeneous among the individual cells, before resuming growth when encounter a growth-supportive condition[4–6]. The lag time is associated with the invasiveness of pathogens and antibiotic tolerance[7–10]. Recently, it has been suggested that an extended lag time correlated to an increased tolerance towards antibiotics and this 'tolerance by lag' may further facilitate the subsequent evolution of antibiotic resistance[11,12]. Nevertheless, it remains poorly understood on how and why a heterogeneous lag time exists before they recover, mainly due to the low density or inert metabolic activities for these cells.

Here, we discovered a reversible subcellular structure and termed it as the quiescent body, which sequesters selected essential proteins and is formed in the non-growing/non-dividing late stationary-phase *E. coli* cells but is dissolved when the cells resume growth in fresh medium. We further demonstrated that the degree of quiescent body formation is strongly correlated with the duration of lag time for bacterial cells to recover, and it apparently functions as a biological timer for the growth resumption of such non-growing bacterial cells.

The finding of quiescent body was made accidentally by us while performing the unnatural amino acid-mediated protein photo-crosslinking analysis to decipher the assembling pattern of the cell division protein FtsZ, a homolog of the eukaryotic tubulin protein[13,14] and whose monomers are known to self-associate into fibrous protofilaments by using two longitudinal interfaces under *in vitro* conditions[15,16], in living *E. coli* cells. Such protofilaments are believed to further assemble, via an undefined manner, into the Z-ring structure in the middle of each cell before generating constriction during cytokinesis[17,18]. While commonly performed our *in vivo* protein photo-crosslinking analysis on FtsZ in the actively dividing log-phase cells, we once did a similar analysis on the non-dividing late stationary-phase cells, assuming that the FtsZ protein would exist as monomers in them. We found, strikingly, that a large portion of the FtsZ monomers in the late stationary-phase cells, though indeed no longer self-assemble into protofilaments, exist in the insoluble pellet fraction of the cell lysates. We subsequently demonstrated by live-cell imaging analysis that the FtsZ proteins in late stationary-phase cells largely exist in a type of cell-pole granules which also contain many other functionally important proteins. We then revealed that when such non-dividing cells were inoculated in fresh culture

medium, the cell-pole granules, which we termed as quiescent bodies, were effectively dissolved in the re-growing cells, with the sequestered FtsZ protein being relocated into the Z-ring structure. By contrast, those cells that maintained their quiescent bodies intact did not initiate their re-growth, thus displaying a significantly longer lag time. Notably, we found that both the formation (upon entering the stationary phase) and dissolution (during the recovery) occur in a highly heterogeneous manner among the individual cells.

The quiescent body that we unveiled here apparently acts as a biomarker for an efficient and unequivocal identification of the hitherto elusive dormant or persister bacterial cells. More importantly, they conceivably function as a biological timer that defines the duration of lag time for the non-growing bacterial cells to resume growth.

Results

The FtsZ protein interacts with multiple other proteins and exists in the insoluble pellet fraction of non-dividing late stationary-phase *E. coli* cells.

The determined crystal structure of the FtsZ protofilaments reveals a head-to-tail longitudinal assembling pattern of the FtsZ monomers[19,20]. In light of this structural information, we initially tried to confirm whether or not such observed assembling pattern indeed exists in living *E. coli* cells, and meanwhile to identify other interaction surfaces that would allow such protofilaments to further assemble into the higher-order Z-ring. To this end, we performed a systematic *in vivo* protein photo-crosslinking analysis on FtsZ, as mediated by the genetically incorporated unnatural amino acid p-benzoyl-L-phenylalanine (pBpa)[21,22], which has been routinely and effectively used in our laboratory[23–25]. Among the pBpa variants we prepared, FtsZ-K140pBpa was one in which the residue K140, that is reported to locate at the longitudinal interface[19,26], was replaced by pBpa. We first confirmed that FtsZ-K140pBpa is able to substitute the wild-type FtsZ protein in supporting cell division (**Fig. S1A**), ruling out any occurrence of major structural disruptions.

To unequivocally demonstrate whether or not the residue K140 indeed resides in the longitudinal assembling surface of FtsZ in living cells, besides heterologously expressing FtsZ-K140pBpa, we also modified the genomic *ftsZ* gene to produce an Avi-tagged FtsZ form, designated as FtsZ-Avi, which can thus be detected by using the streptavidin-alkaline phosphatase conjugate (abbreviated as streptavidin-AP conjugate) that specifically probes the Avi tag. As shown by the blotting results displayed in **Fig. 1A,** such FtsZ dimers were clearly detected in the actively dividing log-phase cells, either as one band probed with streptavidin-AP conjugate (lane 2, red arrow; formed between FtsZ-K140pBpa and FtsZ-Avi), or as a doublet band probed with anti-FtsZ antibodies (lane 6, red and black arrows; the bottom band formed between two FtsZ-K140pBpa monomers). These results confirm that the residue K140 indeed locates at the self-assembling interface of FtsZ to form protofilaments in living cells.

Out of curiosity, we also performed the above photo-crosslinking experiments with the non-dividing/non-growing late stationary-phase cells, assuming that the head-to-tail protofilaments would no longer exist. The results, also displayed in **Fig. 1A**, clearly show that the photo-crosslinked dimer between FtsZ-K140pBpa and FtsZ-Avi became no longer detectable when probed with the streptavidin-AP conjugate (lane 4), indicating that the FtsZ protofilaments are indeed no longer maintained in such cells. However, when probed with antibodies against FtsZ, multiple photo-crosslinked non-dimer products of FtsZ-K140pBpa were detected (**Fig. 1A,** lane 8). This indicates that the FtsZ monomer, although no longer self-associates, now interacts with multiple other proteins via the original longitudinal interface. Apparently, these interactions may prevent the FtsZ monomers to self-associate into the protofilaments in the non-dividing cells.

We next tried to identify the proteins that interact with FtsZ in the late stationary-phase cells. For this purpose, we initially attempted to purify the photo-crosslinked products of FtsZ-K140pBpa (e.g., through immunoprecipitation) before subjecting them to mass spectrometry analysis. During the purification, however, we strikingly found that not only almost all the photo-crosslinked products of FtsZ-K140pBpa but also a large portion of the two types of free FtsZ monomers were detected in insoluble pellet fraction of the cell lysates (**Fig. 1B**, lane 8), while the photo-crosslinked FtsZ dimers and the free FtsZ monomers were both detected in the soluble supernatant (**Fig. 1B**, lane 3), hardly any in the insoluble pellet (**Fig. 1B**, lane 4) fraction of the log-phase cells.

To rule out the possibility that the detection of FtsZ monomers in the pellet fraction was an artifact due to the introduction of the pBpa residue or the Avi tag in the FtsZ protein and/or the UV irradiation, we then analyzed the distribution of the endogenous FtsZ protein in the supernatant and pellet fractions of the late stationary-phase wild-type *E. coli* cells. Our immunoblotting results, displayed in **Fig. 1C**, clearly demonstrate that the endogenous FtsZ protein is similarly detected largely in the pellet fraction (top panel, lane 6) of late stationary-phase cells, with little in the pellet fraction (lane 3) of the log-phase cells. For comparison, we found that EF-Tu (as one of the most abundant proteins) and GroEL (as a molecular chaperone protein that usually interacts with unfolded client proteins) were both detected largely in the supernatant (lane 5), hardly in the pellet (lane 6) of late stationary-phase cells (**Fig. 1C**, middle and bottom panels, respectively). Taken together, these results strongly suggest that the FtsZ proteins apparently exist as insoluble forms in late stationary-phase *E. coli* cells.

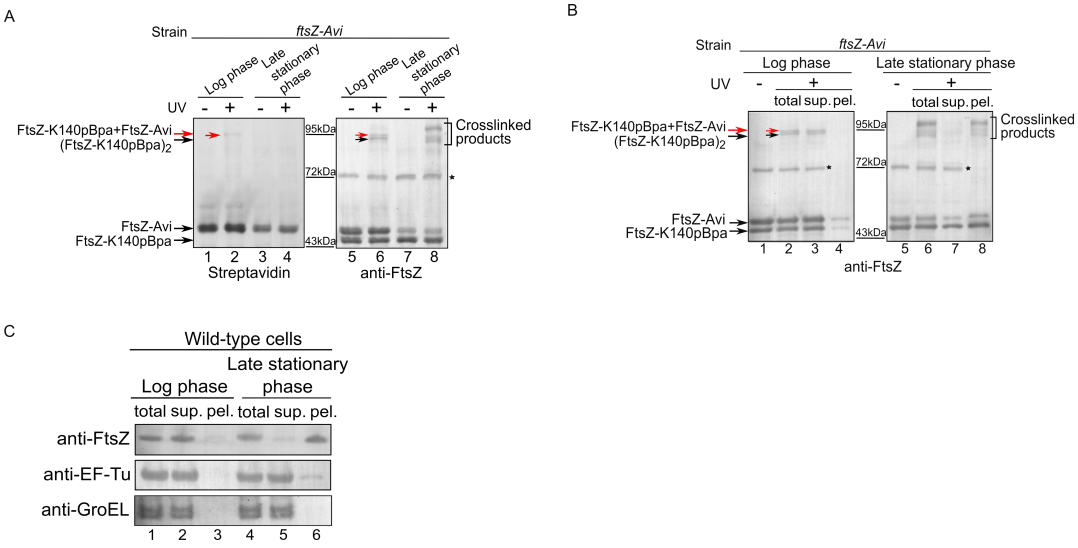

Figure 1. The FtsZ protein is detected in the insoluble pellet fraction of non-dividing late stationary-phase *E. coli* cells.

(A) Blotting results for detecting photo-crosslinked products of the FtsZ-K140pBpa variant in log-phase and late stationary-phase cells of the *ftsZ-Avi* strain, probed with the streptavidin-AP conjugate (Streptavidin) or antibodies against FtsZ protein (Anti-FtsZ). Indicated on the left are positions of the two indicated monomers and the two photo-crosslinked dimers, indicated in the middle are positions of the molecular weight markers, indicated on the right are positions of photo-crosslinked products formed between FtsZ-140pBpa and other non-FtsZ proteins. The asterisk indicates a non-specific protein band generated when probed with the anti-FtsZ antibodies.

(B) Immunoblotting results for detecting the photo-crosslinked products and free monomers in the supernatant (sup.) and pellet (pel.) fractions of the log-phase or late stationary-phase *ftsZ-Avi* cells expressing the FtsZ-K140pBpa variant, probed with antibodies against FtsZ. The asterisk indicates the same non-specific protein band as described in (**A**). Positions of the bands are similarly indicated as in (**A**).

(C) Immunoblotting results for detecting the endogenous FtsZ, EF-Tu or GroEL in the total cell lysate (total), the supernatant (sup.) and the pellet (pel.) fractions of log-phase or late stationary-phase wild-type *E. coli* cells, probed with the indicated antibodies.

It should be pointed out that in late stationary-phase cells a significant amount of the monomers for either FtsZ-K140pBpa or FtsZ-Avi were detected in the supernatant fraction of the transformed *E. coli* cells (panel **B**, lane 7), while the endogenous FtsZ in the wild-type cells are largely detected in the pellet fraction (panel **C**, lane 5). This is most likely due to the fact that the total amount of the FtsZ proteins, as represented by both FtsZ-K140pBpa and FtsZ-Avi, in the transformed cells is significantly higher than that of the endogenous FtsZ in the wild-type cells.

The FtsZ protein exists in cell-pole granules in the late stationary-phase *E. coli* cell.

We next attempted to gain further insight into the status of FtsZ protein in late stationary-phase *E. coli* cells by performing live-cell fluorescence microscopic imaging analysis. For this purpose, we labeled the FtsZ protein with the green fluorescent protein mNeonGreen by generating the FtsZ-mNeonGreen fusion protein and heterologously expressed it in wild-type *E. coli* cells, similar to what was reported before by others[27]. We confirmed, as shown in **Fig. 2A** (top part) that this FtsZ-mNeonGreen fusion protein is effectively incorporated into and thus labels the Z-ring structure in the middle of actively dividing log-phase cells.

We then subjected the late stationary-phase cells to similar live-cell imaging analysis, and revealed, of great interest, that the FtsZ-mNeonGreen proteins were largely detected in two granules that locate at the two cell poles (**Fig. 2A**, bottom part). For comparison, the similarly expressed unfused mNeonGreen protein was found to be evenly distributed in the cytoplasm of either log-phase (top panel) or late stationary-phase (bottom panel) cells (**Fig. S1C**). Subsequent three-dimensional fluorescence imaging analysis (as displayed in **Movie S1)** showed that such cell-pole granules take a shape of ellipsoid (**Fig. 2A**, bottom row, enlarged images) whose ellipticity was calculated to be 0.35 ± 0.065 ($n > 200$). It is pertinent to note that such an ellipsoid shape is dramatically different from the spherical or rod shape as commonly taken by inclusion bodies, being a structure commonly formed by a particular protein that is over-expressed in bacterial cells [28]. Consistent with what we observed above (**Figs. 1B** and **1C**), a majority of either the endogenous FtsZ or the heterologously expressed FtsZ-mNeonGreen was detected in the pellet fraction of the late stationary-phase cells (**Fig. 2B**, lane 6), but in the supernatant fraction of the log-phase cells (**Fig. 2B**, lane 2). Collectively, these results demonstrate that the FtsZ protein in non-dividing late stationary-phase cells no longer exists as the Z-ring structure but as a form of cell-pole granules.

We then tried to further clarify the subcellular localization of such cell-pole granules. For this purposes, we first constructed an *E. coli* strain whose *rhaBAD* gene in the rhamnose operon was replaced by a gene encoding the FtsZ-mNeonGreen protein, such that the expression of the latter is directed by the rhamnose-inducible promoter, as illustrated in **Fig. S1D** (top panel). We verified that the FtsZ-mNeonGreen protein is produced only in the presence of rhamnose (**Fig. S1D**, bottom left panel) and the production of FtsZ-mNeonGreen hardly affected the normal growth of the cells (**Fig. S1D**, bottom right panel). Similarly, the Z-ring in log-phase cells and the cell-pole granules in late stationary-phase cells were observed for the *ftsZ-mNeonGreen* strain when cultured in the presence of rhamnose (**Fig. S1E**).

We then separately labeled the outer membrane with OmpA (an outer membrane protein)-fused red fluorescent protein mCherry[29] (**Fig. 2C**, top panel), the inner membrane with the inner membrane anchoring peptide (derived from the nlpA protein)-fused mCherry[30] (**Fig. 2C**, middle panel) and the cytosol with the unfused mCherry (**Fig. 2C**, bottom panel) in the *ftsZ-mNeonGreen* strain. The live-cell imaging data displayed in **Fig. 2C** clearly show that the cell-pole granules occupy a cytosolic location which is hardly accessible to the cytosolic mCherry proteins (bottom panel), suggesting that the structure of the granules are rather compact. Collectively, these imaging data unequivocally demonstrate that, in late stationary-phase cells, the FtsZ protein largely exists in the compact cell-pole granules with a shape significantly different from that of inclusion bodies.

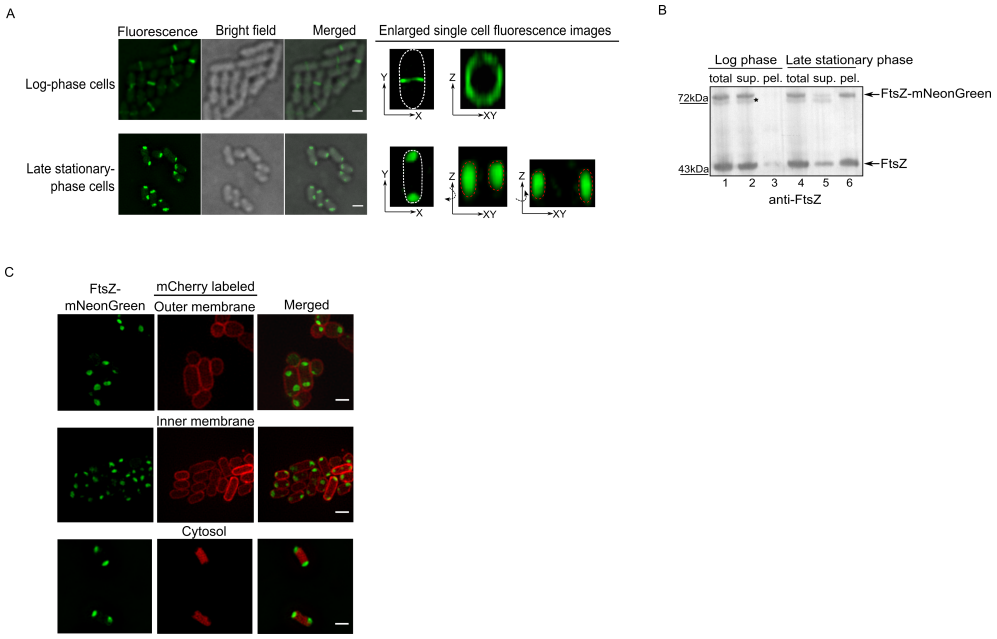

Figure 2. The heterologously expressed FtsZ-mNeonGreen protein exists in a form of cell-pole granules in late stationary-phase *E. coli* cells.

(A) Fluorescence and bright field microscopic images of the log-phase (cultured to 6 h; top panel) and late stationary-phase (cultured to 24 h; bottom panel) *E. coli* cells in which the FtsZ-mNeonGreen protein, besides the endogenous FtsZ protein, was heterologously expressed from a plasmid. Enlarged single cell fluorescent images are also displayed for a better view of the Z-ring structure (in the log-phase cells) and the cell-pole granules (in late stationary-phase cells). Scale bars, 1 μm.

(B) Immunoblotting results for detecting both the endogenous FtsZ and the heterologously expressed FtsZ-mNeonGreen in the total cell lysate (total), supernatant (sup.) and pellet (pel.) fractions of log-phase or late stationary-phase cells, probed with antibodies against FtsZ. Positions of FtsZ and FtsZ-mNeonGreen are indicated on the right and of the molecular weight markers on the left. The asterisk indicates the non-specific protein band.

(C) Fluorescence microscopic images of late stationary-phase *ftsZ-mNeonGreen* cells whose outer membrane (top), inner membrane (middle) or cytosol (bottom) was separately labeled via the fused mCherry (for the two membranes) or unfused mCherry (for the cytosol). Scale bars, 1 μm.

The cell-pole granule or quiescent body selectively sequesters proteins that are vital to cell growth and division.

After searching the literatures, we noticed a report that described the isolation (via sucrose gradient centrifugation) of a multi-protein aggregates which are only formed in stationary-phase *E. coli* cells [31]. However, without a further analysis on the status of the proteins, the authors assumed that such aggregates are made of misfolded proteins and destined for degradation. As a matter of fact, it remains a great challenge to directly demonstrate whether a protein in such insoluble structures is folded or not even under *in vitro* conditions, let alone in living cells. Despite of this, we made an effort to find out whether the FtsZ proteins residing in the cell-pole granules are folded, noting that the FtsZ protein was reported not to form inclusion bodies when over-expressed in bacterial cells[32].

To this end, we again exploited the *in vivo* protein photo-crosslinking analysis mediated by the unnatural amino acid pBpa, assuming that the pBpa variants of FtsZ protein would form photo-crosslinked products with other proteins in a surface-specific manner if it is folded[33]. Specifically, we performed the *in vivo* protein photo-crosslinking in late stationary-phase cells for a number of pBpa variants of FtsZ, which were isolated from a random library that we constructed (details to be described elsewhere).

When probed with streptavidin-AP conjugate (against the Avi tag), the blotting results show that, similar to FtsZ-K140pBpa (**Fig. 1A**, lane 4), none of these pBpa variants formed photo-crosslinked FtsZ dimers (results for 11 of them are displayed in **Fig. S2A**) in late stationary phase cells. When the same samples were probed with antibodies against FtsZ, as shown in **Fig. 3A**, we found that the pBpa variants of the FtsZ protein interact with other particular proteins apparently in a surface specific fashion. Specifically, for example, when pBpa was placed at residue position 151, 166 or 174 (**Fig. 3A**, lanes 2, 4 and 6), all of which occupy a spatial position adjacent to K140 according to the determined crystal structure of FtsZ monomer[34], a pattern of photo-crosslinked products largely comparable to that of FtsZ-K140pBpa was revealed (**Fig. 1A**, lane 8). Similarly, the four variants with pBpa introduced at position 31, 47, 51 or 54, all of which are adjacent to each other but distant from K140, also generated a pattern of photo-crosslinked products similar to each other but different from that of FtsZ-K140pBpa (**Fig. 3A**, lanes 8, 10, 12 and 14). In contrast, the variants with pBpa at the rest positions (**Fig. 3A**, lanes 16, 18, 20, 22, 24, 26 and 28), each occupying a non-adjacent spatial position, generated no or individually unique patterns of crosslinked products. Collectively, these observations indicate that the FtsZ proteins in the cell-pole granules of late stationary-phase cells are apparently folded.

We next attempted to find out whether or not such cell-pole granules could maintain their structure and thus be isolated as intact entities after the cells are lysed. The imaging results shown in **Fig. 3B** clearly demonstrate that such granules could still be clearly detected in the cell lysates. We subsequently collected the granules as the centrifugation pellet of the lysed wild-type *E. coli* cells and then re-suspended it in 8 M urea to effectively dissolve the protein components within them, before the large membrane fragments to be removed as the new pellet through another round of centrifugation. Afterwards, the new supernatant was concentrated by about 10-fold before the sample was resolved by SDS-PAGE. The Coomassie blue staining results, displayed in **Fig. 3C**, revealed many protein bands (lane 10), with a pattern apparently different from that of the total cell lysates (lane 5), suggesting that the protein components present in the cell-pole granules are selected. This meanwhile demonstrate that the protein composition of the cell-pole granules is clearly distinguishable from that of the inclusion body, which is commonly composed of several dominant proteins that are heterologously over-expressed[28].

We subsequently excised the protein bands that could be clearly visualized on the gel for mass spectrometry analysis. As listed in **Fig. 3D**, besides FtsZ, numerous key proteins that are known to function in such fundamental biological processes as transcription, translation, metabolism and cell division were identified. We verified the presence of five of these identified proteins, by separately expressing each as an Avi-tagged form from a plasmid construct, in the pellet fraction of late stationary-phase and in the supernatant fraction of log-phase cells, as shown in **Fig. 3E** (lanes 6 vs 3).

Our live-cell imaging analysis, performed by fusing the target protein with mNeonGreen, also verified the presence of FtsA and ZapC, two proteins that we identified in the cell-pole granules and are known to function in cell division[27,35], in Z-ring structure of log-phase cells but in cell-pole granules of late stationary-phase cells (**Fig. S2B**). By contrast, FtsL and ZapA, two proteins that we did not identify in the cell-pole granules but are also known[36] and confirmed by us to be present in the Z-ring structure of log-phase cells, were found to be evenly distributed in the cytoplasm, rather than in the cell-pole granules, in late-stationary phase cells (**Fig. S2B**). In addition, we demonstrated that FtsA (fused with the red fluorescent protein mCherry) co-localizes with FtsZ (fused with mNeonGreen), not only in the Z-ring structure of log-phase cells but also in the cell-pole granules either in late stationary-phase cells or in their lysates, as shown in **Fig. S2C**. Taken together, these observations suggest that the cell-pole granules apparently sequester selected proteins which are important for cell growth and division. In view that the cell-pole granules are only formed in the non-growing/non-dividing late-stationary phase bacterial cells, we hereafter designate them as “quiescent bodies” and continue to explore their biological significance by utilizing FtsZ-mNeonGreen as the biomarker.

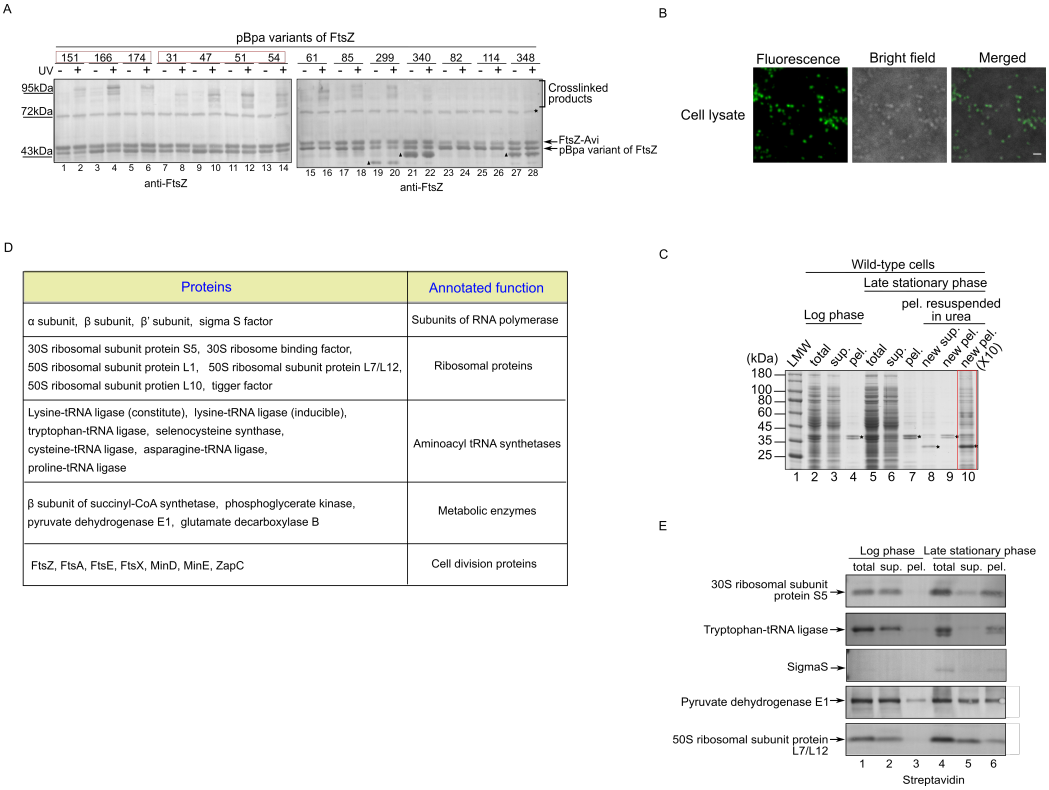

D

Proteins	Annotated function
α subunit, β subunit, β' subunit, sigma S factor	Subunits of RNA polymerase
30S ribosomal subunit protein S5, 30S ribosome binding factor, 50S ribosomal subunit protein L1, 50S ribosomal subunit protein L7/L12, 50S ribosomal subunit protien L10, tigger factor	Ribosomal proteins
Lysine-tRNA ligase (constitute), lysine-tRNA ligase (inducible), tryptophan-tRNA ligase, selenocysteine synthase, cysteine-tRNA ligase, asparagine-tRNA ligase, proline-tRNA ligase	Aminoacyl tRNA synthetases
β subunit of succinyl-CoA synthetase, phosphoglycerate kinase, pyruvate dehydrogenase E1, glutamate decarboxylase B	Metabolic enzymes
FtsZ, FtsA, FtsE, FtsX, MinD, MinE, ZapC	Cell division proteins

Figure 3. The cell-pole granules (quiescent bodies) selectively sequester proteins essential for cell growth and division.

(A) Immunoblotting results for detecting the photo-crosslinked products of the indicated pBpa variants of FtsZ in late stationary-phase *ftsZ-Avi* cells, as probed with antibodies against FtsZ. The asterisk indicates a non-specific protein band, and the triangles indicate the truncated forms of FtsZ produced due to the failure of pBpa incorporation at the replaced TAG stop codon.

(B) Fluorescence and bright field microscopic images of the cell-pole granules as detected in lysates of late stationary-phase (cultured to 24 h) cells in which the FtsZ-mNeonGreen protein was heterologously expressed in addition to the endogenous FtsZ.

(C) Coomassie blue-stained SDS-PAGE results for detecting proteins present in the total lysate (lanes 2 and 5), supernatant (lanes 3 and 6) and pellet fractions (lanes 4 and 7) of log-phase or late stationary-phase wild-type *E. coli* cells. The pellet of the lysate (as analyzed in lane 7) of late stationary-phase cells was dissolved in 8 M urea and re-centrifuged, with the new supernatant (new sup.; lane 8) being concentrated by approximately 10-fold before loaded for the gel electrophoresis (lane 10). Asterisks (in lanes 4 and 7-10) indicate the protein bands that were identified by mass spectrometry analysis as outer membrane proteins OmpA, OmpF and OmpC, which apparently ended in the pellet fraction as large outer membrane fragments that were generated during cell lysis by French Press.

(D) List of major proteins that were identified in the quiescent body-containing insoluble pellet by mass spectrometry analysis.

(E) Blotting results for analyzing the distribution of the indicated proteins, that were identified in the quiescent bodies and linked with an Avi tag, in the indicated fractions of log-phase or late stationary-phase wild-type *E. coli* cells, probed with streptavidin-AP conjugate against the Avi tag. Of note, the sigma S factor was previously reported only to be accumulated in late stationary-phase but not in log-phase bacterial cells[37].

Quiescent bodies are formed in a heterogeneous manner among individual cells.

Before our effort to identify the factors that trigger the formation of quiescent bodies, we first examined the time course of quiescent body formation during cell culturing. For this purpose, we monitored the status of the FtsZ protein by performing live-cell imaging analysis with the *ftsZ-mNeonGreen* cells cultured to particular time

points from 6 h (log-phase) to 24 h (late-stationary phase) and in the presence of rhamnose (to induce the production of the FtsZ-mNeonGreen protein).

The data displayed in **Fig. 4** reveal, remarkably, that the formation of quiescent bodies appears to be highly heterogeneous among individual cells. Specifically, at the 12 h culturing point, although the Z-ring structure became no longer visible in many cells, quiescent bodies are not yet visible in them. At the 15 h culturing point, although the Z-ring structure remained visible in some of the cells, quiescent bodies started appearing in many of the rest. At the 18 h culturing point, the Z-ring structure became no longer visible and the quiescent bodies appeared almost in all the cells. At the 21 h culturing point, quiescent bodies appear to be fully formed in all the cells. The heterogeneity of quiescent body formation is most clearly indicated by the imaging data recorded at the 15 h point, when the Z-ring structures remain visible in some of the cells while quiescent bodies are well formed in some others. Additionally, quiescent body formation seems to first start at one cell pole rather than start simultaneously at both poles in each individual cell and that each quiescent body appears to be formed in a multi-stage and progressive manner.

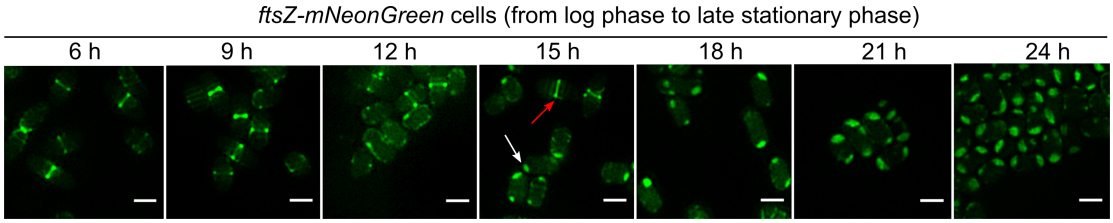

Figure 4. The formation of quiescent bodies appears to be highly heterogeneous among individual *E. coli* cells.
Fluorescence microscopic images of the *ftsZ-mNeonGreen* cells recorded at the indicated time points of culturing. Cells were grown in Luria-Bertani (LB) medium containing 0.02% rhamnose. Scale bars, 1 μm.

Formation of quiescent bodies could be effectively induced in log-phase cells that are placed in the late stationary-phase culture medium or induced by indole.

The fact that quiescent bodies start to be formed in the cells only until certain culturing points strongly suggests that their formation is triggered due to the accumulation of certain signaling molecules produced by the cells themselves during their culturing in the Luria-Bertani medium. This is somehow analogous to the effect of the quorum sensing signaling molecules that are accumulated in the culture medium when the cell density reaches a certain level[38]. We then assessed whether or not the culture medium derived from late stationary phase (of 24 h culturing) is able to induce the formation of quiescent bodies in the actively dividing log-phase cells (of 6 h culturing). Data presented in **Fig. 5A** (top panel) reveal that the Z-ring structure started to disappear after the log-phase cells were placed in the late-stationary phase culture medium for as short as 1 hour, with quiescent bodies to be fully formed almost in all the cells after approximately 4 hours. As a control, the Z-ring structure was

clearly visible in all the untreated cells after a parallel culturing for the same duration (**Fig. 5A**, bottom panel). These results indicate that certain factor, likely produced by the normal metabolic activities of the cells, was accumulated and induced the formation of quiescent bodies.

It has been documented that the catabolism of amino acids will proceed after the sugars are exhausted for bacterial cells cultured in LB medium[39]. This leads to accumulation of certain metabolic products such as ammonia and indole in the culture medium[39–41]. In light of this, we then examined whether ammonia or indole is able to substitute the late stationary-phase culture medium in inducing the formation of quiescent bodies in log-phase cells. We demonstrated that ammonia appears to be ineffective in inducing the formation of quiescent bodies in log-phase cells. By contrast, quiescent bodies became clearly visible in log-phase cells that were treated, for example, with 5 mM indole for as short as 1 hour, or 2.5 mM indole for 2 hours (**Fig. 5B**). In line with this, the FtsZ protein was significantly detected in the pellet fraction of such indole-treated log-phase cells (**Fig. 5C**, lane 6). Nevertheless, we found that quiescent bodies could still be effectively formed in late stationary-phase cells lacking the *tnaA* gene, which encodes the tryptophanase enzyme that is believed to be responsible for producing indole from L-tryptophan in bacterial cells[40,42] (**Fig. S3**). These results indicate that indole, though effective in inducing the formation of quiescent bodies in log phase cells, is still apparently not the essential factor for the formation of quiescent bodies in stationary-phase cells.

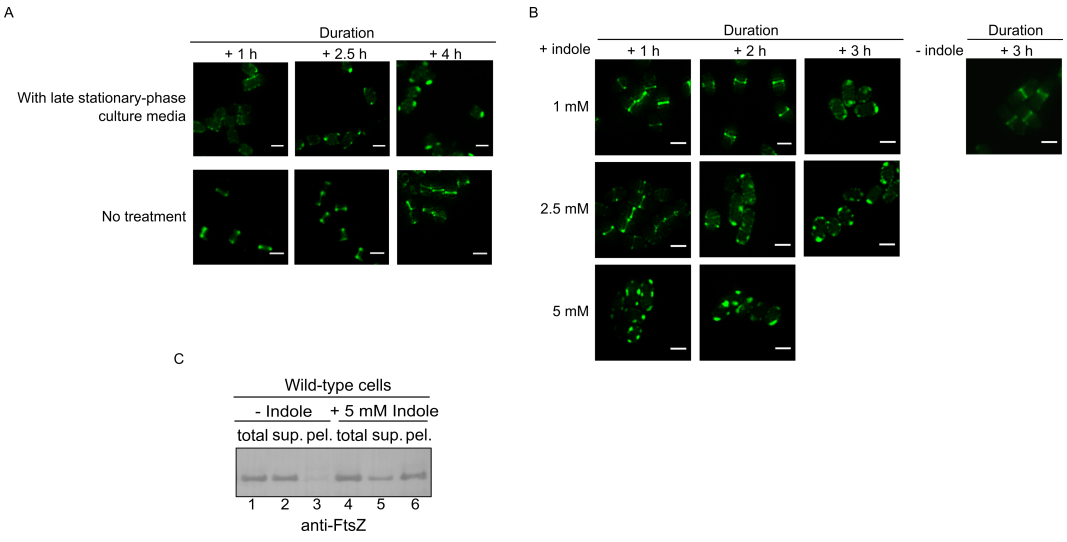

Figure 5. Late stationary-phase LB culture medium or indole is able to effectively induce the formation of quiescent bodies in log-phase *E. coli* cells.

(A) Fluorescence microscopic images of log-phase *ftsZ-mNeonGreen* cells that were placed in late stationary-phase LB culture medium for the indicated duration (top panel). The untreated log-phase cells that were further cultured were analyzed here as the negative control (bottom panel). Scale bars, 1 μm.

(B) Fluorescence microscopic images of log-phase *ftsZ-mNeonGreen* cells that were treated with indole (+ indole) of the indicated concentrations and durations. As the negative control (- indole), the cells were treated with DMSO (the solvent used for dissolving indole). Scale bars, 1 μm.

(C) Immunoblotting results for detecting the presence of FtsZ in the total cell lysate (total, lane *4*), supernatant (sup., lane 5) or pellet (pel., lane 6) fraction of the log-phase wild-type cells that were

treated with indole (5 mM) for 1 h, as probed with antibodies against FtsZ. Untreated cells (-indole) were analyzed here as the negative control (lanes 1-3).

Formation of quiescent bodies relies on the operation of cellular respiration.

During the experiments described above (**Fig. 5B**), we accidentally noticed that a sufficient supply of oxygen is critical for indole to exhibit its inducing effect. Specifically, quiescent bodies would not be formed in the log-phase cells if the induction was performed in airtight tubes and without shaking, as shown in **Fig. 6A** (the - O_2 image). Given that indole was reported to be able to dissipate the proton gradient across the inner membrane in *E. coli* cells [43], such an inducing effect of indole might be due to its acceleration of the electron transferring process, which would rely on an adequate supply of oxygen. This speculation is partly supported by our observation that the inducing effect of indole on quiescent body formation would be eliminated in the presence of glucose, whose metabolism was known to inhibit cellular respiration[41,44], in the culture medium before the log-phase cells were treated with indole even in a sufficient supply of oxygen (**Fig. 6A**; the + O_2, + Glc image**)**.

We then assessed whether the occurrence of cellular respiration is essential for quiescent body formation in bacterial cells. For this purpose, we examined whether or not quiescent body formation will be affected either in the *ftsZ-mNeonGreen* (for the imaging analysis shown in **Fig. 6B**) or in wild-type (for the immunoblotting analysis shown in **Fig. 6C**) strain in which either the *nuoA* or *sdhC* gene was knocked down by using the CRISPRi technology[45]. The results, as shown in **Fig. 6B** (right column images), revealed that the formation of quiescent body hardly occurs in the *sdhC* knockdown or rarely in the *nuoA* knockdown late-stationary phase cells. Consistently, formation of quiescent bodies no longer occurs in the log-phase cells of either the *sdhC* or *nuoA* knockdown strain that were treated with indole (**Fig. 6B**, middle column images). In line with this failure of quiescent body formation, the immunoblotting data, shown in **Fig. 6C**, indicate that little endogenous FtsZ protein was detected in the pellet fraction (lanes 6 or 9) of the late stationary-phase *nuoA* or *sdhC* knockdown cells. Taken together, these observations indicate that the normal operation of cellular respiration is essential for the formation of quiescent bodies in bacterial cells. It should be pointed out that we achieved similar results with the *nouAB* or *sdhCDAB* knockout *E. coli* mutant strain.

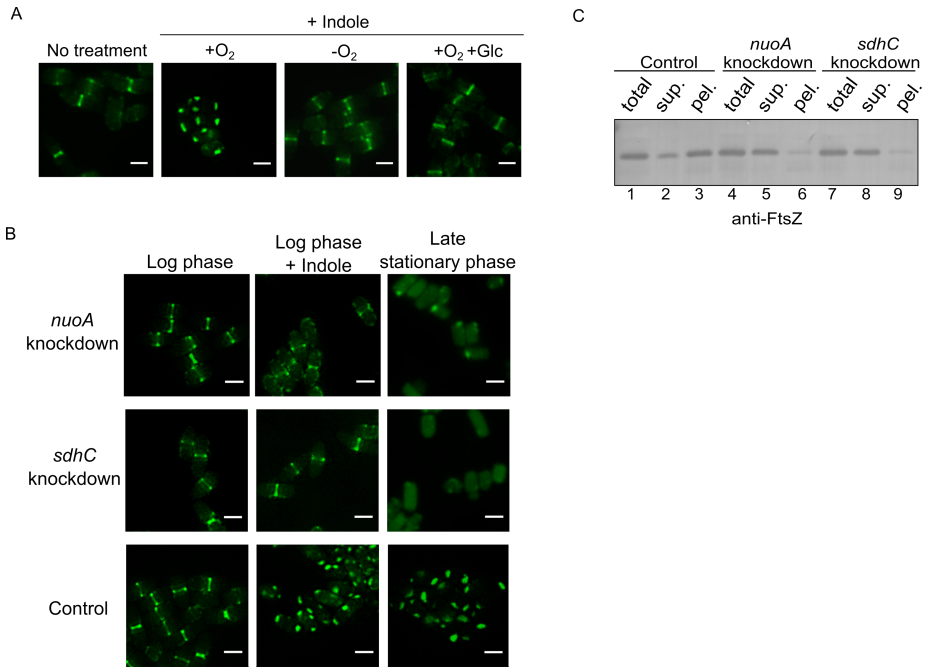

Figure 6. Normal operation of cellular respiration is essential for the formation of quiescent bodies.

(A) Fluorescence microscopic images of log-phase *ftsZ-mNeonGreen* cells that were treated with indole (5 mM) for 1 h, under the indicated conditions of oxygen and glucose supplies. Scale bars, 1 μm.

(B) Fluorescence microscopic images of log-phase (untreated or treated with indole) or late stationary-phase *ftsZ-mNeonGreen* cells possessing a knockdown of the *nuoA* or *sdhC* gene. For the control, a non-targeting crRNA (CRISPR RNA) was expressed in the *ftsZ-mNeonGreen* cells. Scale bars, 1 μm.

(C) Immunoblotting results for detecting the distribution of FtsZ in the indicated fractions of late stationary-phase *nuoA*- or *sdhC*-knockdown cells, probed with anti-FtsZ antibodies.

Quiescent bodies are dissolved in a highly heterogeneous manner among individual cells with the FtsZ protein being re-utilized to form the Z-ring structure when late stationary-phase cells are re-cultured in fresh medium.

We subsequently tried to gain insight on the biological significance of the quiescent body. To this end, we first examined the fate of the quiescent bodies when the late stationary-phase *ftsZ-mNeonGreen* cells were placed in fresh culture medium. Live-cell imaging data shown in **Fig. 7A** indicate, intriguingly, that when re-cultured in fresh LB medium lacking rhamnose (thus no new FtsZ-mNeonGreen protein would be synthesized), a time-dependent relocation of the FtsZ-mNeonGreen protein from the quiescent bodies to the Z-ring structure was clearly observed as soon as a cell starts to re-grow (marked by an increase in size; as represented by the two cells circled with white lines). By contrast, quiescent bodies remained unaltered in cells that had not yet started their re-growth (marked by a lack of size increase; as represented by the two cells circled with red lines in **Fig. 7A**).

The remarkable reversible nature of the FtsZ proteins sequestered in the quiescent bodies was further verified. Specifically, the immunoblotting results, shown in **Fig. 7B**, demonstrate that while the FtsZ protein detected in the pellet fraction of wild-type

(not the *ftsZ-mNeonGreen*) cells became gradually reduced (lanes 3 to 6 to 9), those detected in the supernatant fraction became gradually increased (lanes 2 to 5 to 8), during the re-culturing of the late stationary-phase cells. In line with this, we also observed a time-dependent increase in the level of photo-crosslinked FtsZ-K140pBpa homo-dimers, accompanied with a parallel decrease in the level of the photo-crosslinked products between FtsZ-K140pBpa and other proteins (lanes 2-4, **Fig. 7C**) in the cells that were re-cultured in fresh LB medium lacking pBpa (thus no new FtsZ-K140pBpa protein would be synthesized). Taken together, these observations reveal that the proteins (as represented by FtsZ) sequestered in quiescent bodies could be released for functional resumption when the late stationary-phase cells re-grow and re-divide in fresh medium.

Interestingly, the live-cell imaging data of the *ftsZ-mNeonGreen* cells, as displayed in **Fig. 7A**, also clearly demonstrate that the dissolution of quiescent bodies, analogous to their formation (as shown in **Fig. 4**), also occurs in a highly heterogeneous manner among individual cells. It is conceivable that such a heterogeneity in their formation and dissolution are related in a certain way. For example, the formation of quiescent bodies in each stationary-phase cell apparently occurs in multiple consecutive stages such that those more mature ones may take longer time to initiate their dissolution. It follows that the time taken for the quiescent bodies to initiate their dissolution in each bacterial cell may correspond to the lag time during cell recovery[6,39,46].

We next examined whether or not the FtsZ proteins in the quiescent bodies could be released when the synthesis of all proteins is suppressed by the presence of the antibiotic chloramphenicol [47]. The live-cell imaging data shown in **Fig. 7D** reveal a similar time-dependent disappearance of the FtsZ-mNeonGreen protein in quiescent bodies in the cells that initiated their re-growth (e.g., the two white circled cells). With no exception, the heterogeneity phenomenon of quiescent body dissolution was once again clearly observed here (one non-growing cell whose quiescent bodies remain unaltered is indicated by the red circled cell in **Fig. 7D**). Again, immunoblotting results, displayed in **Fig. 7E**, clearly reveal a similar solubility change of the FtsZ protein as observed above (**Fig. 7B**) during the re-culturing of the wild-type (not the *ftsZ-mNeonGreen*) cells. These observations suggest that the dissolution of quiescent bodies apparently does not rely on new protein synthesis and thus qualifies as an early event for non-growing bacterial cells to recover.

Collectively, the data displayed in **Fig. 7** suggest that the proteins sequestered in quiescent bodies can be effectively released to resume their functions upon cell re-growth/re-division, and that the lag time during the recovery of non-growing bacterial cells apparently reflect the time taken for the quiescent bodies to initiate their dissolution (as further demonstrated below).

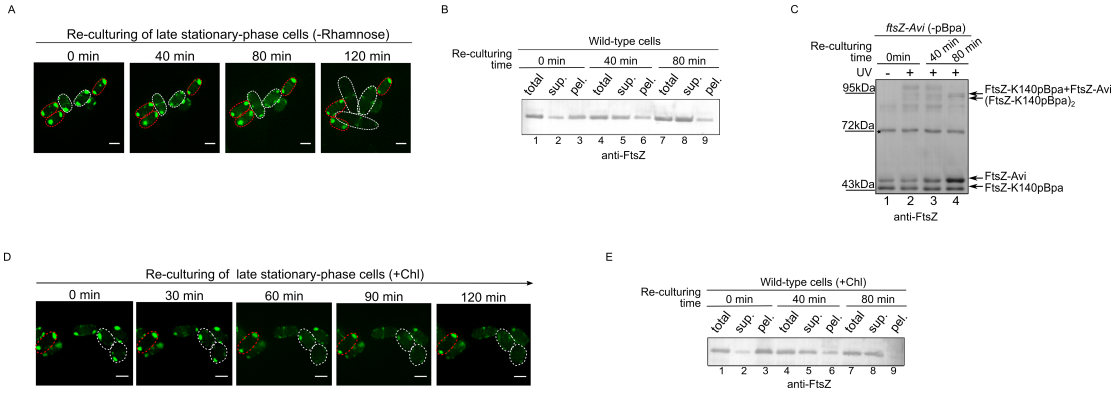

Figure 7. The quiescent bodies are dissolved in a highly heterogeneous manner among individual cells upon their re-growth/re-division releasing the sequestered FtsZ proteins that are re-utilized in forming the Z-ring structure.

(A) Live-cell fluorescence microscopic images of late stationary-phase *ftsZ-mNeonGreen* cells that were re-cultured to the indicated time points in fresh LB medium lacking rhamnose. The cells indicated by red circles did not start their re-growth while those indicated by white circles started their re-growth during the 120 min of re-culturing. (Note: one of the re-growing cells divided into two daughter cells at the 120 min re-culturing time point). Scale bars, 1 μm.

(B) Immunoblotting results for detecting the distributions of FtsZ in the supernatant (sup.) and pellet (pel.) fractions of the late stationary-phase wild-type (not the *ftsZ-mNeonGreen*) cells that were re-cultured in fresh LB medium to the indicated time points, probed with anti-FtsZ antibodies.

(C) Immunoblotting results for detecting the photo-crosslinked products of FtsZ-K140pBpa expressed in the late stationary-phase *ftsZ-Avi* cells that were re-cultured to the indicated time points in fresh LB medium lacking pBpa, probed with antibodies against FtsZ. Indicated on the right are positions of the FtsZ monomers, being FtsZ-K140pBpa and FtsZ-Avi, and the photo-crosslinked FtsZ dimers, being $(FtsZ\text{-}K140pBpa)_2$ and FtsZ-K140pBpa+FtsZ-Avi.

(D) Live-cell fluorescence microscope images (recorded at 37^{o}C) of the late stationary-phase *ftsZ-mNeonGreen* cells that were inoculated to the indicated time points in fresh LB medium containing the antibiotic chloramphenicol which inhibits the overall protein synthesis in the cells. Two cells whose quiescent bodies were dissolving are indicated by the white circles; one cell whose quiescent bodies remained unaltered during the 120 min of re-culturing is indicated by the red circle. Scale bars, 1 μm.

(E) Immunoblotting results for detecting the distributions of the FtsZ protein in the indicated fractions when the late stationary-phase wild-type (not the *ftsZ-mNeonGreen*) cells were re-cultured to the indicated time points in fresh LB medium containing chloramphenicol, probed with anti-FtsZ antibodies.

The degree of quiescent body formation in the non-growing cells is correlated with the duration of the lag time for their re-growth.

We next tried to find out whether or not the duration of lag time for the bacterial cell recovery can be correlated to the degree of quiescent body formation in the non-growing cells. For this purpose, we decided to make use of the multiple types of *E. coli* cells that form quiescent bodies to different degrees, as described above (**Figs. 4**, **5B** and **6B**). Additionally, we decided to express their lag time as the average initial doubling time upon re-division (abbreviated as re-division T_{id}), which was calculated on the basis of their re-culturing growth curves (displayed in **Fig. S5**).

The lag time measurement results of the multiple types of cells, described in **Figs. 8A-8C**, reveal a strong correlation between the duration of lag time and the degree of

quiescent body formation (as shown in **Figs. 4**, **5B** and **6B**) in the recovering bacterial cells. First, as shown in **Fig. 8A**, the re-division T_{id} value is increased by about 3 fold for cells pre-cultured for 24 h (being ~108 min) when compared with cells pre-cultured for 12 h (being ~34 min). It should be pointed out that the re-division T_{id} value of the cells pre-cultured for 12 h was largely comparable with that of the log-phase cells (being ~26 min; equivalent to the "- indole, + O_2" bar in **Fig. 8B**). Second, as shown in **Fig. 8B**, the re-division T_{id} value of the indole-treated log-phase cells (the "+ indole, + O_2" bar) was about 2.5 fold (~65 min vs ~26 min) of that of the non-treated cells (the "- indole, + O_2" bar). Third, as shown in **Fig. 8C**, the difference in re-division T_{id} values between the late stationary phase (24 h culturing) and the early stationary phase (12 h culturing) cells for either the *nuoA* or *sdhC* knockdown strain was much less**,** when compared with that for the wild type control cells (in which a non-targeting CRISPR RNA was transcribed). Fourth, as also shown in **Fig. 8C**, for the *sdhC* knockdown strain (in which quiescent bodies no longer form), the re-division T_{id} value of its late stationary-phase cells is not higher but largely comparable with that of its early stationary-phase cells.

Consistently, we also observed a strong correlation between the degree of quiescent body formation and the level of antibiotic tolerance. For instance, as shown in **Fig. 8D**, we demonstrated that the survival rate of the indole-treated log-phase *E. coli* cells (the "+ indole, + O_2" bars), in which quiescent bodies were effectively formed, was approximately 10-fold higher than that of the untreated cells (the "- indole, + O_2" bars) when inoculated in fresh medium containing either ofloxacin or ampicillin. Similarly, as shown in **Fig. 8E**, the survival rate of the quiescent body-lacking stationary-phase *sdhC*-knockdown cells was approximately 50-fold lower than that of the stationary-phase wild-type cells in which a non-targeting crRNA was expressed (the "control" bars). Likewise, the survival rate of the *nuoA*-knockdown cells was approximately 5-fold lower than that of the control cells (**Fig. 8E**).

In line with the observations on lag time and antibiotic tolerance, our live-cell imaging analysis with the *ftsZ-mNeonGreen* cells, as shown in **Fig. 8F**, revealed that only cells (e.g., the two circled by white lines) whose quiescent bodies became dissolved were eventually killed after a swelling (i.e., became invisible at a certain time point after an increase in their sizes) in the presence of ampicillin during the re-culturing process. By contrast, the cells (e.g., the one circled by red lines in **Fig. 8F**) whose quiescent bodies maintained intact remained unaltered (i.e., remained visible in their original sizes at all the time points) during such re-culturing process. These results meanwhile suggest that the quiescent body probably can be viewed as a biomarker to label the unawakened cells during bacterial re-culturing process.

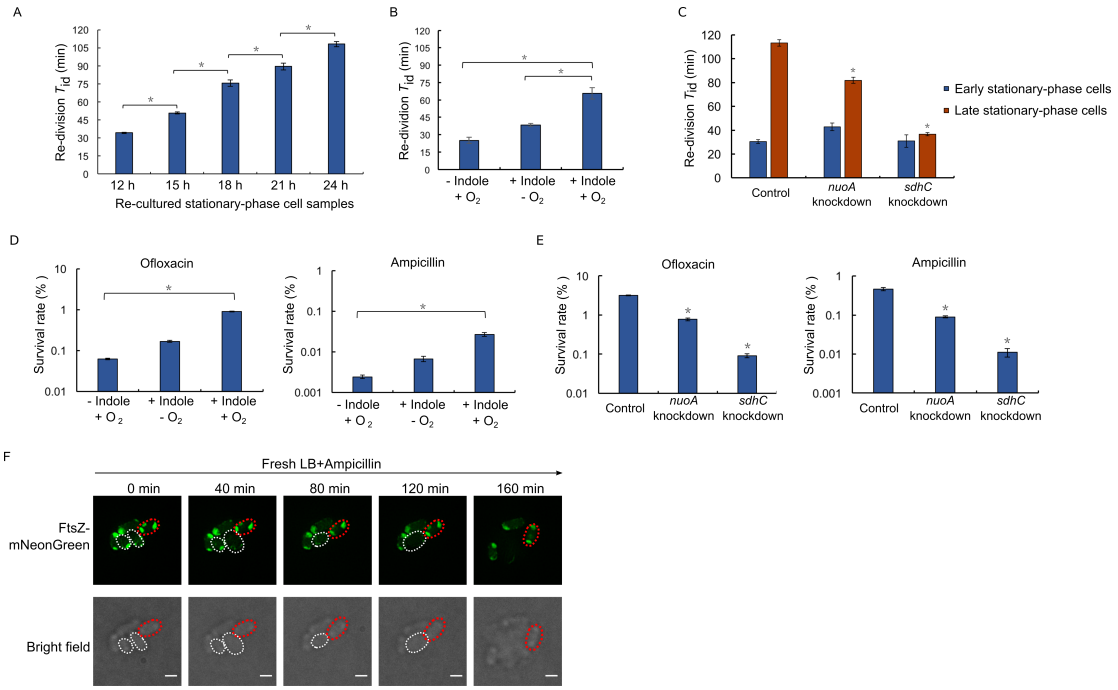

Figure 8. The degree of quiescent body formation in the non-growing bacterial cells is correlated with the duration of the lag time for their recovery.

(A) The re-division T_{id} of wild-type stationary-phase cells that were pre-cultured to the indicated time points. The cells were re-cultured (after diluting 40-fold) at 37℃ in fresh LB medium. The re-division T_{id} values were calculated based on the increase in cell number within the first 30 min of the re-culturing cells (for details, see Methods).

(B) The re-division T_{id} values of wild-type log-phase cells that were untreated (- indole) or treated (+ indole) with indole (5 mM, 1 h) and having an adequate (+ O_2) or limited (- O_2) oxygen supplies.

(C) The re-division T_{id} values of early (blue bars) or late (red bars) stationary-phase wild-type (control; in which a non-targeting crRNA was transcribed from a plasmid) and the *nuoA* or *sdhC* knockdown cells.

(D) Survival rates of wild-type log-phase cells that were untreated (- indole) or treated (+ indole) with indole, and with the adequate (+ O_2) or limited (- O_2) oxygen supply before subsequently re-cultured in fresh LB medium containing ofloxacin (5 μg/ml) or ampicillin (200 μg/ml). The survival rates were calculated as: [colony-forming units of the antibiotic-treated cells] / [colony-forming units of the antibiotic-untreated cells] ×100.

(E) Survival rates of the late stationary-phase wild-type (control), *nuoA*- or *sdhC*-knockdown cells that were re-cultured in fresh LB medium containing the indicated antibiotics. Again, a non-targeting crRNA was transcribed from a plasmid in the control cells.

The symbol '＊' in all the above panels indicates a significant difference between the compared pair of samples (P-value <0.01, t-test). At least three replicates were performed for each measurement.

(F) Live-cell fluorescence (top) or bright field (bottom) microscopic images of the late stationary-phase *ftsZ-mNeonGreen* cells that were re-cultured at 37 ℃ in fresh ampicillin-containing LB medium to the indicated time points. The re-growing cells (which were eventually lysed after a swelling, thus became invisible at a certain time point) and non-growing cells (which maintained their sizes unaltered and quiescent bodies intact all through the re-culturing process) are indicated by the white and red circles, respectively. Scale bars, 1 μm.

Discussion

Here, we accidentally discovered a new reversible subcellular structure that termed as the quiescent body in *E. coli* cells. This structure is formed only in

non-growing/non-dividing late stationary-phase cells and initiates to dissolve when the cells re-grow/re-divide in fresh culture medium. We suppose that such a novel structure is also similarly formed in other bacterial species. In retrospect, these findings were made apparently as a result of our unique approach, *in vivo* protein photo-crosslinking in combination with live-cell imaging, as well as our focusing on the unique FtsZ protein, which assembles into the Z-ring structure.

Our major observations can be briefly summarized as follows. First, *in vivo* protein photo-crosslinking analysis revealed that the FtsZ protein, although exists as homo-oligomers in actively dividing log-phase cells, dissociates into monomers, which interacts with other proteins and was detected in the pellet fraction of non-dividing late stationary-phase cells (**Fig. 1**). Second, live-cell imaging analysis confirmed that the FtsZ protein indeed no longer exists as the Z-ring structure, but meanwhile unveiled that it exists in two cell-pole granules in each late stationary-phase cell (**Fig. 2**). Third, mass spectrometry analysis revealed that such cell-pole granules selectively sequester proteins (including FtsZ) that are vital for cell growth and division (**Fig. 3**), and we thus named them as quiescent bodies. Fourth, further live-cell imaging analysis of cells cultured to different time points showed that the quiescent bodies are gradually formed in a highly heterogeneous manner among individual cells (**Fig. 4**). Fifth, we demonstrated that the formation of quiescent bodies can be effectively induced in log-phase cells that were placed in the late stationary-phase culture medium or were treated with indole (**Fig. 5**). Sixth, gene knockdown (and knockout) studies in combination with live-cell imaging analysis indicated that the formation of quiescent bodies relies on the operation of cellular respiration (**Fig. 6**). Seventh, live-cell imaging in combination with *in vivo* protein photo-crosslinking analysis demonstrated that when the non-dividing/non-growing cells were re-cultured in fresh medium, quiescent bodies can be dissolved independent on protein biosynthesis, also in a heterogeneous manner among individual cells, allowing the released proteins to resume their functions (**Fig. 7**). Eighth, our analysis on the average re-division initial doubling time (re-division T_{id} values) as well as the survival rate towards antibiotic treatments demonstrated that the degree of quiescent body formation is highly correlated with the duration of lag time for the non-growing bacterial cells to recover (**Fig. 8**).

One major implication of these findings is that the quiescent body apparently functions as a biological timer for a non-growing bacterial cell to resume growth, as indicated by the following observations. First, quiescent body formation among individual cells appears to be highly heterogeneous such that it begins at different time points in different cells and that it takes multiple stages for their maturation in each cell during the culturing (**Fig. 4**). Second, the dissolution of quiescent bodies also occurs in a highly heterogeneous manner among individual cells such that it occurs in some cells at a very early time point while remain intact in some others even at a very late time point during the re-culturing (**Fig. 7A**). Third, the duration of lag time for the re-culturing is strongly correlated to the degree of quiescent body

formation such that the re-division T_{id} value is higher for cells that are derived from a later stage of the stationary phase (**Fig. 8A**). The role of quiescent body as a biological timer for bacterial cell growth resumption is apparently reflected as such that the initiation of the dissolution of "younger" quiescent bodies occurs more efficiently and thus takes less time, while that of the "older" ones occurs less efficiently and thus takes longer time. In other words, the differential formation and dissolution of quiescent bodies in individual cells may follow a "last-in-first-out (or first-in–last-out)" rule[48]. The heterogeneous forming and dissolving processes of quiescent bodies are schematically illustrated in **Fig. 9**.

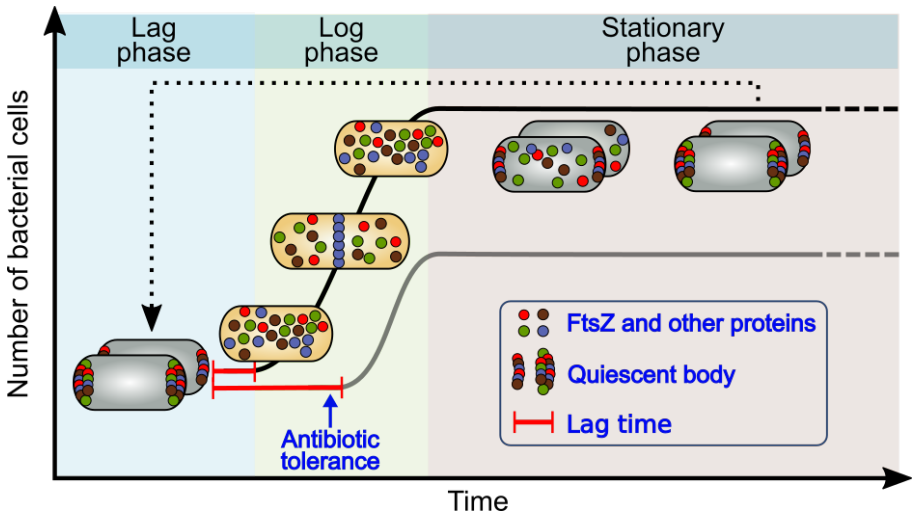

Figure 9. The quiescent body, that is formed in the non-growing stationary phase bacterial cells and is dissolved in the recovering cells, functions as a biological timer for non-growing bacterial cells to resume growth.

It has long been recognized that when bacteria are cultured in the laboratory, there always exists a lag phase, in which cell growth is hardly appreciable before the cells resume their growth from the non-growing state[6]. The status of the cells in this lag phase remains poorly understood mainly due to their lack of metabolic activities. Our discoveries reported here for the first time unveiled the occurrence of such a key cellular event as the initiation of the dissolution of quiescent bodies in this unique recovering stage of the bacterial cells. Their dissolution apparently does not rely on new protein synthesis, thus qualifies as an early event for non-growing bacterial cells to recover. By the same token, given that multiple proteins essential for cell growth and division are largely sequestered in the quiescent bodies, their formation probably locks the cells in a non-growing state. It follows that the dissolution of quiescent bodies and the release of these key proteins represent a major barrier that the cells have to overcome during the lag phase before they can initiate their re-growing process.

The heterogeneous nature of quiescent body formation and dissolution among individual cells, that would in turn generate a heterogeneity in the duration of lag time taken by individual cells before their recovery, might provide a bet-hedging strategy

for the survival of the bacterial species[12,49,50]. Specifically, due to such heterogeneities, under any particular environmental condition, only a certain portion of the non-growing cells would initiate the dissolution of their quiescent bodies and thus resume their growth. Such recovered cells, though may generate more offspring if the condition is optimal, would become vulnerable and might be killed if the condition suddenly becomes adverse again. By contrast, those cells that maintain their quiescent bodies and thus remain non-growing, although not to contribute to any offspring, would be highly tolerant towards the adverse conditions and thus important for preventing the species from becoming extinct.

It has been long recognized that the dormant (persister) cells exist in an extremely low number and possess an appearance hardly distinguishable from the non-dormant (non-persister) ones in the bacterial cell population[2,51]. These obstacles have prevented an effective investigation on them before we can find a feasible way to eradicate them. In view of our findings reported here, we suppose that the formation of quiescent bodies is a far more reliable distinguishable feature for defining dormant (persister) bacterial cells, in comparison with the commonly described non-growing/non-dividing feature[2,3]. We observed in this study that the wild-type cells cultured to 12 h or the *sdhC*-knockdown cells cultured to 24 h, both of which do not possess quiescent bodies although in a non-growing/non-dividing state, are able to re-grow and re-divide immediately without displaying a lag time, when placed in fresh LB medium (**Figs. 8A** and **8C**, respectively). This implicate that the non-growing/non-dividing feature is not a reliable one for defining dormant (persister) bacterial cells. Additionally, it has been commonly believed that many bacterial species collected from the natural environment exist in a "viable but non-culturable" state [52,53]. It is certainly worth future investigation to find out whether the presence of quiescent bodies is also a common and distinguishing feature of such non-growing/non-dividing bacterial cells.

Much needs to be further clarified on the biology of quiescent bodies. For example, first, what is the chemical composition of the quiescent body and what other molecules are present in addition to the proteins we identified? Second, how the chemical components in the quiescent bodies are organized? Third, what is (are) the key signal molecule (s) that directly trigger their formation in the stationary-phase cells and how such signals are sensed by the cells to initiate the molecular events leading to their formation? Fourth, why is the operation of cellular respiration essential for their formation? Fifth, how are the proteins sequestered in them specifically selected? Sixth, what signals trigger the initiation of their dissolution when the cells are exposed to growth-permissive conditions and what are the molecular events leading to their dissolution? Last but not least, we need to find out whether a similar structure is present in eukaryotic cells.

METHODS

Bacterial strains, plasmids and genome modifications. Phenotypes of the bacterial strains, all derived from the *E. coli* BW25113 strain, are listed in **Table S1**. The plasmids used in this study are all listed in **Table S2**. All the genomic modifications (to generate the *ftsZ-mNeonGreen*, *ftsZ-Avi*, Δ*nuoAB*, or Δ*sdhCDAB* strain) were –red genomic recombination system[54]. All the newly generated plasmids and genomic modifications were confirmed by DNA sequencing.

Bacterial cell culturing. Luria Bertani (LB) liquid (10 g/l tryptone, 5 g/l yeast extract and 5 g/l NaCl) or agar-containing solid culture medium was sterilized by autoclaving. g/ml ampicillin was added to the culture medium. Log-phase and late stationary-phase cells refer to those that were cultured at 37℃ in test tubes shaking at 260 r.p.m for 6 h and 24 h, respectively, after the overnight-cultured cells were diluted 100-fold dilution in LB fresh medium.

***In vivo* protein photo-crosslinking of the pBpa variants of FtsZ.** This is performed by using a *ftsZ* conditional knockout strain, named as LY928-Δ*ftsZ* (pJSB100), which we constructed based on the LY928 strain whose genome contains the genes encoding the orthogonal amino acyl-tRNA and tRNA, both needed for incorporating unnatural amino acid pBpa [22], as we described earlier (22). In the LY928-Δ*ftsZ* (pJSB100) strain, the wild-type FtsZ protein is expressed from the pJSB100 plasmid upon arabinose induction [55]. For analyzing complementation capacity of a certain pBpa variant of FtsZ, another plasmid that constitutively expressing it was transformed into the LY928-Δ*ftsZ* (pJSB100) strain. Such transformed cells were then cultured in parallel g/ml ampicillin and 0.05% arabinose) and in the so-called glucose repression medium M pBpa). A variant was considered to be complement the wild-type FtsZ if the transformed cells were able to grow not only in the induction medium but also in the repression medium (to be non-complement if only to grow in the former, not in the latter). For performing the photo-crosslinking analysis, each pBpa variant of FtsZ was expressed in the self-constructed LY928-*ftsZ*-Avi strain (in which an Avi Tag was fused to the C-terminus of the endogenous wild type FtsZ protein), and the cells were M pBpa. The cells were then irradiated with UV light (365 nm) for 10 min at room temperature by using a Hoefer UVC 500 Crosslinker (Amersham Biosciences) and collected by centrifugation at 13,000 × *g* before subjecting to blotting analysis.

Fluorescence microscopic imaging. Cell or cell lysate samples were dropped onto a glass dish (NEST biotechnology, USA) and covered with agar before micrographs were acquired at 37°C (for the re-culturing cell samples) or at 30°C (for all other samples) with an N-SIM imaging system (Nikon) by using the 2D-SIM mode, with a 100×/1.49 NA oil-immersion objective (Nikon) and being excited by a 488 nm or 561 nm laser beam. The 3D images were acquired with an N-SIM and a Deltavision OMX SR (GE Healthcare) imaging system by using the 3D mode. The samples were sectioned at the Z-axis every 120 nm or 240 nm. The images were further reconstructed by using the NIS-Elements AR 4.20.00 (Nikon) and the Imaris software

before further processed with the GNU image manipulation program. The oblate is calculated using the Imaris software. At least 4 images were taken and more than 50 bacterial cells were examined for each experiment. All experiments were independently repeated for at least 3 times.

Cellular fraction separation. The late stationary-phase *E. coli* cells were prepared by growing the cells at 37℃ (shaking at 260 r.p.m.) for 24 h after the overnight-cultured cells were diluted 100-fold into fresh LB medium. The cell samples in re-culturing experiments (as shown in **Fig. 7B**, **7E**) were prepared by transferring the 2-fold diluted late stationary-phase cells into fresh LB medium in the absence or presence of g/ml) and further cultured at 37℃ (shaking at 260 r.p.m.) to a particular indicated time point. The cells were then collected by centrifugation (8000 × *g*) and disrupted by a French press at 1000 MPa before centrifuged at 13,000 × *g* to separate the supernatant and pellet.

Blotting analysis. The samples including cell lysate, supernatant fraction, pellet fraction and the cells irradiated to UV were each added into the sample buffer, boiled and analyzed by tricine SDS-PAGE, or further probed with the indicated antibodies or streptavidin-AP conjugate for blotting analysis. The visualized protein bands on gels were scanned and processed using the GNU image manipulation program.

CRISPRi experiments. These were performed according to previously reported methods [45]. Briefly, plasmids carrying the crRNA that targets the *nuoA* or *sdhC* gene were transformed into the *E. coli* cells in which the proteins for recognizing and binding specific DNA sequences are expressed from the Cascade operon and the gene (*cas3* gene) encoding the protein that cleaves the target sequence was deleted. The designed DNA sequences for knocking down the *nuoA* and the *sdhC* genes were ATAGCGAATGCCCAGTGATGAGCGATGACTTC and AATGTGAAAAAACAAAGACCTGTTAATCTGGA, respectively. The control plasmid carried a non-targeting crRNA sequence CTGCTGGAGCTGGCTG CAAGGCAAGCCGCCCA. The crRNAs on the plasmids are transcribed constitutively, rather being induced.

Cell re-growth and calculation of the average initial doubling time upon re-division (re-division T_{id}). Log-phase or late stationary-phase cells of a particular type were diluted 40-fold into fresh LB medium and cultured at 37℃ with shaking (260 r.p.m.). Growth curves were prepared by measuring the OD_{600} value of the cultured cells at 30 min intervals. The re-division T_{id} value was calculated as 30 / $log_2^{Nt1/Nt0}$ min, where N_{t0} and N_{t1} are the number of cells at 0 min and 30 min, respectively. The N_{t1}/N_{t0} ratio for each batch of cultured cells was calculated based on the increase in optical density at 600 nm (the correlation between the cell number and the OD_{600} value was determined by preparing a standard curve).

Assay for cell survival after antibiotic treatment. Late stationary-phase cells or indole-induced log-phase cells were diluted 40-fold into fresh LB medium containing g/ml ampicillin and incubated at 37℃ with shaking (260 r.p.m.) for 2 h. The cells were then collected by centrifugation (to remove the culture medium and the antibiotics), re-suspended in phosphate-buffered saline (PBS) and serially diluted in PBS before being spotted on LB agar plates for Colony Formation Unit (CFU) counting. The cell survival rate was calculated as: [number of colonies formed after antibiotics treatment] / [number of colonies formed without antibiotic treatment] ×100.

Acknowledgments

We thank Harold P. Erickson (Duke University, USA) for kindly providing us the plasmid pJSB100 and Peter G. Schultz (The Scripps Research Institute, USA) for providing us the plasmids carrying genes encoding the orthogonal tRNA and amino acyl-tRNA for incorporating pBpa into target proteins. We thank Keio Collections for providing us the wild-type *E. coli* strain. We thank the Core Facilities at the School of Life Sciences, Peking University, for assistance in using the structured illumination microscopy (SIM), and we are grateful to Drs. Chunyan Shan and Xiaochen Li for their kind help in performing the fluorescence microscopic imaging analysis. We thank Dr. Wen Zhou at the Mass Spectrometry Facility of the National Center for Protein Sciences at Peking University for assistance in performing the mass spectrometry analysis. We thank Prof. Xinmiao Fu from Fujian Normal University for useful discussions. This work was supported by funds from the National Natural Science Foundation of China (No. 31670775 and 31470766 to ZYC), the National Basic Research Program of China (No. 2012CB917300 to ZYC) and Qidong-SLS Innovation Fund.

Author Contributions

Jiayu Yu and Yang Liu designed and performed the experiments, analyzed the data and drafted the manuscript. Prof. Zengyi Chang supervised this study and edited the manuscript.

Conflict of Interest

We declare that we have no conflicts of interest related to this work.

References

1352 1. Bigger, J. TREATMENT OF STAPHYLOCOCCAL INFECTIONS WITH
1353 PENICILLIN BY INTERMITTENT STERILISATION. *The Lancet* **244,** 497–500
1354 (1944).
1355 2. Burke, V., Sprague, A. & Barnes, L. V. Dormancy In Bacteria. *J. Infect. Dis.* **36,**
1356 555–560 (1925).
1357 3. Lewis, K. Persister cells, dormancy and infectious disease. *Nat. Rev. Microbiol.* **5,**
1358 48–56 (2007).
1359 4. Levin-Reisman, I. *et al.* Automated imaging with ScanLag reveals previously
1360 undetectable bacterial growth phenotypes. *Nat. Methods* **7,** 737–739 (2010).
1361 5. Monod, J. The Growth of Bacterial Cultures. *Annu. Rev. Microbiol.* **3,** 371–394
1362 (1949).
1363 6. Penfold, W. J. On the Nature of Bacterial Lag. *J. Hyg. (Lond.)* **14,** 215–241 (1914).
1364 7. Hathaway, L. J. *et al.* Capsule type of Streptococcus pneumoniae determines
1365 growth phenotype. *PLoS Pathog.* **8,** e1002574 (2012).
1366 8. Frimodt-Møller, N., Sebbesen, O. & Frølund Thomsen, V. The pneumococcus and
1367 the mouse protection test: importance of the lag phase in vivo. *Chemotherapy* **29,**
1368 128–134 (1983).
1369 9. Bättig, P., Hathaway, L. J., Hofer, S. & Mühlemann, K. Serotype-specific
1370 invasiveness and colonization prevalence in Streptococcus pneumoniae correlate with
1371 the lag phase during in vitro growth. *Microbes Infect.* **8,** 2612–2617 (2006).
1372 10. Brauner, A., Fridman, O., Gefen, O. & Balaban, N. Q. Distinguishing between
1373 resistance, tolerance and persistence to antibiotic treatment. *Nat. Rev. Microbiol.* **14,**
1374 320–330 (2016).
1375 11. Levin-Reisman, I. *et al.* Antibiotic tolerance facilitates the evolution of resistance.
1376 *Science* eaaj2191 (2017). doi:10.1126/science.aaj2191
1377 12. Fridman, O., Goldberg, A., Ronin, I., Shoresh, N. & Balaban, N. Q. Optimization
1378 of lag time underlies antibiotic tolerance in evolved bacterial populations. *Nature* **513,**
1379 418–421 (2014).
1380 13. Dai, K. & Lutkenhaus, J. ftsZ is an essential cell division gene in Escherichia coli.
1381 *J. Bacteriol.* **173,** 3500–3506 (1991).
1382 14. Erickson, H. P. Atomic structures of tubulin and FtsZ. *Trends Cell Biol.* **8,**
1383 133–137 (1998).
1384 15. Erickson, H. P., Taylor, D. W., Taylor, K. A. & Bramhill, D. Bacterial cell division
1385 protein FtsZ assembles into protofilament sheets and minirings, structural homologs of
1386 tubulin polymers. *Proc. Natl. Acad. Sci. U. S. A.* **93,** 519–523 (1996).
1387 16. Mukherjee, A. & Lutkenhaus, J. Analysis of FtsZ Assembly by Light Scattering
1388 and Determination of the Role of Divalent Metal Cations. *J. Bacteriol.* **181,** 823–832
1389 (1999).
1390 17. Erickson, H. P., Anderson, D. E. & Osawa, M. FtsZ in Bacterial Cytokinesis:
1391 Cytoskeleton and Force Generator All in One. *Microbiol. Mol. Biol. Rev.* **74,** 504–528
1392 (2010).

18. Romberg, L. & Levin, P. A. Assembly Dynamics of the Bacterial Cell Division Protein FtsZ: Poised at the Edge of Stability. *Annu. Rev. Microbiol.* **57,** 125–154 (2003).
19. Matsui, T. *et al.* Structural reorganization of the bacterial cell-division protein FtsZ from Staphylococcus aureus. *Acta Crystallogr. D Biol. Crystallogr.* **68,** 1175–1188 (2012).
20. Oliva, M. A., Cordell, S. C. & Löwe, J. Structural insights into FtsZ protofilament formation. *Nat. Struct. Mol. Biol.* **11,** 1243–1250 (2004).
21. Chin, J. W., Martin, A. B., King, D. S., Wang, L. & Schultz, P. G. Addition of a photocrosslinking amino acid to the genetic code of Escherichiacoli. *Proc. Natl. Acad. Sci. U. S. A.* **99,** 11020–11024 (2002).
22. Ryu, Y. & Schultz, P. G. Efficient incorporation of unnatural amino acids into proteins in Escherichia coli. *Nat. Methods* **3,** 263–265 (2006).
23. Fu, X., Shi, X., Yan, L., Zhang, H. & Chang, Z. In Vivo Substrate Diversity and Preference of Small Heat Shock Protein IbpB as Revealed by Using a Genetically Incorporated Photo-cross-linker. *J. Biol. Chem.* **288,** 31646–31654 (2013).
24. Wang, Y. *et al.* A Supercomplex Spanning the Inner and Outer Membranes Mediates the Biogenesis of β-Barrel Outer Membrane Proteins in Bacteria. *J. Biol. Chem.* **291,** 16720–16729 (2016).
25. Zhang, M. *et al.* A genetically incorporated crosslinker reveals chaperone cooperation in acid resistance. *Nat. Chem. Biol.* **7,** 671–677 (2011).
26. Li, Y. *et al.* FtsZ protofilaments use a hinge-opening mechanism for constrictive force generation. *Science* **341,** 392–395 (2013).
27. Ma, X., Ehrhardt, D. W. & Margolin, W. Colocalization of cell division proteins FtsZ and FtsA to cytoskeletal structures in living Escherichia coli cells by using green fluorescent protein. *Proc. Natl. Acad. Sci. U. S. A.* **93,** 12998–13003 (1996).
28. Rinas, U. *et al.* Bacterial Inclusion Bodies: Discovering Their Better Half. *Trends Biochem. Sci.* (2017). doi:10.1016/j.tibs.2017.01.005
29. Verhoeven, G. S., Dogterom, M. & den Blaauwen, T. Absence of long-range diffusion of OmpA in E. coli is not caused by its peptidoglycan binding domain. *BMC Microbiol.* **13,** 66 (2013).
30. Harvey, B. R. *et al.* Anchored periplasmic expression, a versatile technology for the isolation of high-affinity antibodies from Escherichia coli-expressed libraries. *Proc. Natl. Acad. Sci. U. S. A.* **101,** 9193–9198 (2004).
31. Kwiatkowska, J., Matuszewska, E., Kuczyńska-Wiśnik, D. & Laskowska, E. Aggregation of Escherichia coli proteins during stationary phase depends on glucose and oxygen availability. *Res. Microbiol.* **159,** 651–657 (2008).
32. Mukherjee, A. & Lutkenhaus, J. Purification, assembly, and localization of FtsZ. *Methods Enzymol.* **298,** 296–305 (1998).
33. Mori, H. & Ito, K. Different modes of SecY-SecA interactions revealed by site-directed in vivo photo-cross-linking. *Proc. Natl. Acad. Sci. U. S. A.* **103,** 16159–16164 (2006).

34. Löwe, J. & Amos, L. A. Crystal structure of the bacterial cell-division protein FtsZ. *Nature* **391,** 203–206 (1998).
35. Durand-Heredia, J. M., Yu, H. H., De Carlo, S., Lesser, C. F. & Janakiraman, A. Identification and Characterization of ZapC, a Stabilizer of the FtsZ Ring in Escherichia coli. *J. Bacteriol.* **193,** 1405–1413 (2011).
36. Ghigo, J. M. & Beckwith, J. Cell division in Escherichia coli: role of FtsL domains in septal localization, function, and oligomerization. *J. Bacteriol.* **182,** 116–129 (2000).
37. Zhou, Y. & Gottesman, S. Regulation of Proteolysis of the Stationary-Phase Sigma Factor RpoS. *J. Bacteriol.* **180,** 1154–1158 (1998).
38. Waters, C. M. & Bassler, B. L. Quorum sensing: cell-to-cell communication in bacteria. *Annu. Rev. Cell Dev. Biol.* **21,** 319–346 (2005).
39. Sezonov, G., Joseleau-Petit, D. & D'Ari, R. Escherichia coli Physiology in Luria-Bertani Broth. *J. Bacteriol.* **189,** 8746–8749 (2007).
40. Gaimster, H. & Summers, D. Regulation of Indole Signalling during the Transition of E. coli from Exponential to Stationary Phase. *PLOS ONE* **10,** e0136691 (2015).
41. Wolfe, A. J. The Acetate Switch. *Microbiol. Mol. Biol. Rev.* **69,** 12–50 (2005).
42. Hopkins, F. G. & Cole, S. W. A contribution to the chemistry of proteids. *J. Physiol.* **29,** 451–466 (1903).
43. Chimerel, C., Murray, A. J., Oldewurtel, E. R., Summers, D. K. & Keyser, U. F. The Effect of Bacterial Signal Indole on the Electrical Properties of Lipid Membranes. *ChemPhysChem* **14,** 417–423 (2013).
44. Basan, M. *et al.* Overflow metabolism in Escherichia coli results from efficient proteome allocation. *Nature* **528,** 99–104 (2015).
45. Luo, M. L., Mullis, A. S., Leenay, R. T. & Beisel, C. L. Repurposing endogenous type I CRISPR-Cas systems for programmable gene repression. *Nucleic Acids Res.* **43,** 674–681 (2015).
46. Novick, A. Growth of Bacteria. *Annu. Rev. Microbiol.* **9,** 97–110 (1955).
47. Wolfe, A. D. & Hahn, F. E. Mode of action of chloramphenicol IX. Effects of chloramphenicol upon a ribosomal amino acid polymerization system and its binding to bacterial ribosome. *Biochim. Biophys. Acta BBA - Nucleic Acids Protein Synth.* **95,** 146–155 (1965).
48. Jõers, A. & Tenson, T. Growth resumption from stationary phase reveals memory in *Escherichia coli* cultures. *Sci. Rep.* **6,** srep24055 (2016).
49. Balaban, N. Q. Persistence: mechanisms for triggering and enhancing phenotypic variability. *Curr. Opin. Genet. Dev.* **21,** 768–775 (2011).
50. Beaumont, H. J. E., Gallie, J., Kost, C., Ferguson, G. C. & Rainey, P. B. Experimental evolution of bet hedging. *Nature* **462,** 90–93 (2009).
51. Lewis, K. Persister Cells. *Annu. Rev. Microbiol.* **64,** 357–372 (2010).
52. Xu, H. S. *et al.* Survival and viability of nonculturableEscherichia coli andVibrio cholerae in the estuarine and marine environment. *Microb. Ecol.* **8,** 313–323 (1982).

53. Li, L., Mendis, N., Trigui, H., Oliver, J. D. & Faucher, S. P. The importance of the viable but non-culturable state in human bacterial pathogens. *Front. Microbiol.* **5,** 258 (2014).

54. Lee, D. J. *et al.* Gene doctoring: a method for recombineering in laboratory and pathogenic Escherichia coli strains. *BMC Microbiol.* **9,** 252 (2009).

55. Stricker, J. & Erickson, H. P. In Vivo Characterization of Escherichia coli ftsZ Mutants: Effects on Z-Ring Structure and Function. *J. Bacteriol.* **185,** 4796–4805 (2003).